Comparative Medicine
Copyright 2020
by the American Association for Laboratory Animal Science

Vol 70, No 3
June 2020
Pages 266–276

Case Report

Retrospective Study of Intercalated Disk Defects Associated with Dilated Cardiomyopathy, Atrial Thrombosis, and Heart Failure in BALB/c Mice Deficient in IL4 Receptor α

Alfonso S Gozalo,[1,*] Patricia M Zerfas,[2] William R Elkins,[1] and Richard L Gieseck III[3]

An increased incidence of dilated cardiomyopathy and atrial thrombosis was noted in a breeding colony of BALB/c mice deficient in IL4 receptor α. The condition affected mice of both sexes and of various ages, and extensive testing (microbiology, serology, histopathology) failed to ascertain the cause. Transmission electron microscopy of heart samples showed structural defects in the myocardial intercalated disks, characterized by unorganized and heavily convoluted arrangement with lower density and less prominent desmosomes and adherens junctions, widening of the intercellular space, myofibrillar lysis adjacent to intercalated disks, occasional sarcomere lysis with marked myofiber degeneration, vacuolation, accumulation of cell debris, and myelin figures. The intercalated disk contains cell adhesion molecules that form cell junctions, allowing contraction coupling of cardiomyocytes and the electrical and mechanical connection between cardiac fibers. Thus, defects at this level result in poor myocardial contraction, intracardiac blood stagnation, and consequently cardiac dilation with clinical signs of heart failure. The background strain or, potentially, the Cre–loxP-mediated recombination system used to create these mice may have contributed to the elevated incidence of cardiomyopathy and atrial thrombosis in this colony. Due to the backcrossing breeding scheme used, we cannot discount the emergence and colonywide dissemination of a spontaneous mutation that affects the intercalated disk. This report underscores the importance of carefully monitoring genetically modified mice colonies for unexpected phenotypes that may result from spontaneous or unintended mutations or enhanced strain background pathology.

DOI: 10.30802/AALAS-CM-19-000059

In humans, dilated cardiomyopathy is often considered an idiopathic disease, but research increasingly shows that the condition has a genetic basis and is collectively known as familial dilated cardiomyopathy.[29] More than 40 individual gene mutations have been identified that contribute to this condition.[29] The affected genes encode various proteins related to the structure and function of cardiomyocytes, severely compromising normal heart function.[29] In mice, dilated cardiomyopathy is occasionally observed in older animals, with some strains appearing to be more susceptible than others.[79] Several lines of genetically engineered mice have been created to study the human disease, most of them with mutations in genes encoding sarcomeric proteins (e.g., α-kinase 3–deficient mice, myosin-binding protein C mutant mice, mice that overexpress tropomodulin, dystrophin- and utrophin-deficient mice, dystrophin and skeletal muscle-specific transcription factor *MyoD*–deficient mice, γ-sarcoglycan–deficient mice, δ-sarcoglycan-deficient mice, muscle LIM protein-deficient mice, desmin-deficient mice, *Mylk3*–deficient mice, Nexilin-deficient mice, and mice with Nebulette mutations)[1,5,15,18,34-36,38,44,45,59,61,67,72,93,96,97] or with mutations that affect intracellular calcium regulation (e.g., mice that overexpress calsequestrin in cardiac myocytes, D73N mutant mice)[44,45,48,62,88] or, in some cases, both (that is, myosin regulatory light chain *MYL2*–RLC D94A mutant mice).[41] Other models include transgenic mice with overexpression of G protein-coupled receptors,[22,47] mice with alterations in genes crucial to cardiac muscle development and function,[26,40] mice with dysregulated extracellular matrix such as TIMP-3–deficient mice,[25] and mice with inactivated cardiac mitochondrial DNA gene expression.[51,99] Acquired forms of dilated cardiomyopathy in mice include infectious (e.g., encephalomyocarditis, Coxsackie virus myocarditis, and parvovirus B19),[11,54,60] autoimmune (e.g., α-MyHC–CFA-immunized mice, PD1–receptor-deficient mice),[7,75] and surgically induced myocardial infarct models.[32] A spontaneous rodent model of dilated cardiomyopathy is the Syrian hamster TO2 strain, due to deletion of the δ-sarcoglycan gene.[6,42,43,74,86,87]

In larger animals, dilated cardiomyopathy is a common heritable disease in various dog breeds.[91] It has been described in Irish wolfhounds, Portuguese water dogs, Great Danes, boxer dogs, and Doberman pinschers.[16,69-71,76,77,81,100] In Doberman pinschers, 2 gene mutations, affecting sarcomeric function and intracellular energy production, have been identified.[91] Clinically, in both animals and humans, the condition is characterized predominantly by left ventricular chamber dilation and poor

Received: 22 May 2019. Revision requested: 01 Jul 2019. Accepted: 22 Oct 2019.
[1]Comparative Medicine Branch, National Institute of Allergy and Infectious Diseases, [2]Pathology Service, Office of Research Services, and [3]Immunopathogenesis Section, Laboratory of Parasitic Diseases, National Institute of Allergy and Infectious Diseases, National Institutes of Health, Bethesda, Maryland
[*]Corresponding author. Email: gozaloa@niaid.nih.gov

systolic function, commonly resulting in left-sided congestive heart failure.[29,91] Cardiac arrhythmias, which can precipitate heart failure and death, are a common complication in these patients.[29] In cats, dilated cardiomyopathy has been associated with taurine deficiency and appears to be multifactorial, with a genetic component.[37]

Atrial thrombosis is a common sequelae of cardiomyopathy and most often as a complication of congestive heart failure.[89] Blood stagnation due to impaired systolic function resulting in increased coagulability of blood are the most important factors predisposing to atrial thrombosis.[89] In humans, atrial thrombi in the left atrium are often observed in late stages of mitral valve stenosis, whereas right atrial thrombosis is more typically a result of atrial fibrillation.[89] In domestic animals, atrial thrombosis is uncommon but has been described in cats and dogs.[55,98] In rodents, atrial thrombosis, mostly affecting the left atrium, is common in older Syrian hamsters.[64,65] Age-related myocardial degeneration resulting in heart failure and intracardiac blood stagnation appears to be the main predisposing factors for atrial thrombosis in aged Syrian hamsters.[65] In rats, the incidence of left atrial thrombosis is low and has been reported in older animals.[14,24] In mice, atrial thrombosis has been described affecting several strains, but the highest incidence (maximum, 66%) appears to occur in aged BALB/c female breeders.[28,68] In addition, atrial thrombosis has been reported in C3H/OUJ mice with marked cardiac atrial and ventricular mural mineralization,[23] mice with coagulopathy due to chronic renal disease,[9] mice with systemic amyloidosis,[9] mice exposed to doxorubicin and other drugs and chemicals,[19,30,84,102] mice with viral myocarditis,[52,94,95] mice fed high fat–low protein purified diets,[17,23] mice with copper deficiency,[53] and in genetically modified mice such as CREM-transgene mice,[13] and mice with cardiac overexpression of β_2-adrenergic receptors.[31]

Here we describe an increased incidence of dilated cardiomyopathy and atrial thrombosis associated with defects in myocardial intercalated disks in a genetically modified mouse colony. This report underscores the importance of carefully evaluating and reporting unexpected adverse phenotypes, given that they may not necessarily be associated with the targeted gene editing but with spontaneous or unintended mutations during the creation of the strain or enhanced background strain pathology.

Materials and Methods

The affected strains in the mice colony were *Il4ra*$^{flox/flox}$, *Il4ra*$^{flox/flox}$*Krt19*$^{WT/creERT}$, *Il4ra*$^{flox/flox}$Rosa26$^{Brainbow\text{-}2.1/Brainbow\text{-}2.1}$ *Il4ra*$^{flox/flox}$*Pdgfrb*$^{WT/cre}$ *Il4ra*$^{flox/flox}$*Lgr5*$^{WT/EGFP\text{-}IRES\text{-}creERT2}$ and *Il4ra*$^{flox/flox}$*Krt19*$^{creERT/WT}$ Rosa26$^{tdTomato/tdTomato}$. *Il4ra*$^{flox/flox}$ mice were obtained from Taconic Biosciences (Germantown, NY). The strain was originally created in the laboratory of Dr Frank Brombacher (Max Planck Institute for Immunobiology, Freiburg, Germany). The IL4 receptor α-deficient mice were generated through homologous and site-specific recombination in BALB/c-derived embryonic stem cells by using the Cre–loxP system to disrupt the gene by deleting exons 7, 8, and 9.[73] The resulting mice have a functional phenotype of impaired IL4- and IL13-mediated activity.[73]

Il4ra$^{flox/flox}$*Krt19*$^{WT/creERT}$, *Krt19*^{creERT} mice were obtained from the Jackson Laboratory (stock no. 026925; Bar Harbor, ME) and backcrossed to *Il4ra*$^{flox/flox}$ mice for 3 to 5 generations. *Krt19*^{creERT} mice were created in the laboratory of Dr Guoqiang Gu (Program in Developmental Biology, Department of Cell and Developmental Biology, Vanderbilt University Medical Center, Nashville, TN).[66] *Krt19*^{creERT} mice have a *cre*^{ERT} fusion gene (a Cre recombinase fused to a mouse estrogen receptor ligand-binding domain) inserted upstream of the initiation codon of the keratin 19 (*Krt19*) gene.[66] When these mice are bred with mice having a *loxP*-flanked sequence, tamoxifen-inducible, Cre-mediated recombination results in deletion of the floxed sequences in the Cre-expressing cells of the offspring.[64] *Krt19*^{creERT} knock-in–knock-out mice are used in studies requiring tamoxifen-induced deletion of floxed sequences in KRT19-expressing epithelial cells (https://www.jax.org/strain/026925).[66]

Il4ra$^{flox/flox}$Rosa26$^{Brainbow\text{-}2.1/Brainbow\text{-}2.1}$ Rosa26-CAG-Brainbow2.1/Confetti mice were obtained from Jackson Laboratory (stock no. 013731) and backcrossed to *Il4ra*$^{flox/flox}$ mice for 4 to 6 generations. Rosa26-CAG-Brainbow2.1/Confetti mice were created in the laboratory of Dr Hans Clevers (Hubrecht Institute, Academy of Arts and Sciences, and University Medical Center, Utrecht, the Netherlands) by using a targeting vector containing (from 5′ to 3′) a CAGG promoter, a *loxP* site, a PGK-Neor-pA cassette, and the Brainbow 2.1 construct.[90] The entire construct was inserted between exons 1 and 2 of the Gt(ROSA)26Sor locus via electroporation into 129P2/OlaHsd-derived IB10/E14IB10 embryonic stem cells. Correctly targeted embryonic stem cells were injected into recipient blastocysts and chimeric males were bred with C57BL/6 females to generate the R26R-Confetti colony.[90] Rosa26-CAG-Brainbow2.1/Confetti mice are used to label and distinguish individual/adjacent cells with nuclear localized, membrane-targeted, or cytoplasmic fluorescent proteins in Cre-recombined cells (https://www.jax.org/strain/013731).

Il4ra$^{flox/flox}$*Pdgfrb*$^{WT/cre}$, Pdgfrb-Cre mice were obtained from Taconic Biosciences and backcrossed to *Il4ra*$^{flox/flox}$ mice for 4 to 6 generations. Pdgfrb-Cre mice were generated in the laboratory of Dr Ralf Adams (London Research Institute, United Kingdom) by pronuclear injection of a *Pdgfrb* gene fragment and a cDNA encoding Cre recombinase followed by an SV40 polyadenylation signal.[27] Cre activity of transgenic founders was characterized in a ROSA26 Cre reporter background. Pdgfrb-Cre and Efnb2-conditional mice were bred to generate Efnb2ΔPC–vSMC mutants. Animals had a mixed 129 × C57BL/6 genetic background.[27] Pdgfrb-Cre mice express Cre recombinase under the control of the *Pdgfrb* promoter and permit Cre recombination in pericytes and smooth vascular muscle cells. (https://www.taconic.com/mouse-model/pdgfrb-cre-mouse).

Il4ra$^{flox/flox}$*Lgr5*$^{WT/EGFP\text{-}IRES\text{-}creERT2}$, *Lgr5*$^{EGFP\text{-}IRES\text{-}creERT2}$ mice were obtained from Jackson Laboratory (stock no. 008875) and backcrossed to *Il4ra*$^{flox/flox}$ mice for 5 generations. *Lgr5*$^{EGFP\text{-}IRES\text{-}creERT2}$ mice were created in the laboratory of Dr Hans Clevers (Hubrecht Institute, Academy of Arts and Sciences, and University Medical Center, Utrecht, the Netherlands) by homologous recombination in embryonic stem cells targeting an *EGFP-IRES-creERT2* cassette to the ATG of *Lgr5*.[8] Correctly targeted embryonic stem cells were injected into recipient blastocysts, and chimeric males were bred with C57BL/6 females. Mutant mice were then crossed to EIIa-cre mice (C57BL/6 genetic background; stock no. 003724, Jackson Laboratory) to remove the neo selection cassette.[8] The resulting mice were backcrossed to C57BL/6J for at least 4 generations and then bred with Rosa26-lacZ mice (C57BL/6 genetic background; stock no. 003474, Jackson Laboratory). Mice with both mutations were further backcrossed and later selectively bred to remove the Rosa26-lacZ allele.[8] *Lgr5*$^{EGFP\text{-}IRES\text{-}creERT2}$ mice are useful for studies requiring lineage-tracing or marking Lgr5-expressing stem cells of the small intestine (https://www.jax.org/strain/008875).

Il4ra$^{flox/flox}$*Krt19*$^{creERT/WT}$Rosa26$^{tdTomato/tdTomato}$, *Krt19*$^{creERT/WT}$Rosa26$^{tdTomato/tdTomato}$ mice were donated by the laboratory of Dr Stuart Forbes (Medical Research Council Centre for Regenerative Medicine, University of Edinburgh, United

Kingdom)[57] and backcrossed to *Il4ra*$^{flox/flox}$ mice for 5 generations. Rosa26-tdTomato mice were originally created by the laboratory of Dr Hongkui Zeng (Allen Institute for Brain Science, Seattle, WA)[58] and deposited in Jackson Laboratory (stock no. 007909). Rosa26-tdTomato mice are also known as Ai9 or Ai9$^{RCL-tdT}$ (https://www.jax.org/strain/007909). Ai9 is a Cre reporter allele that has a *loxP*-flanked STOP cassette preventing transcription of a CAG promoter-driven red fluorescent protein variant (tdTomato)—all inserted between exons 1 and 2 of the *Gt(ROSA)26Sor* locus via electroporation of (129S6/SvEvTac × C57BL/6)F1-derived G4 embryonic stem cells.[58] Correctly targeted embryonic stem cells (clone Ai9) were selected, and chimeric males were bred to C57BL/6J females with resulting mice backcrossed to C57BL/6J. These mice are useful as a Cre reporter strain, which expresses tdTomato fluorescence after Cre-mediated recombination (https://www.jax.org/strain/007909).

With the exception of *Lgr5*$^{-EGFP-IRES-CreERT2}$ and *Pdgfrb*-deficient mice whose homozygous offspring are nonviable or die perinatally, all the described strains were viable and fertile (https://www.jax.org/strain/008875).[27] All affected animals were research naïve and had not been exposed to infectious agents, drugs, or chemicals at the time of clinical presentation. In addition, other mice colonies comprising different strains, transgenics, and knockout mice were maintained and bred in the same animal room, but none showed an increased incidence in dilated cardiomyopathy. The animals were housed in an AAALAC-accredited barrier facility as part of several experimental protocols approved by the National Institute of Allergy and Infectious Diseases Animal Care and Use Committee according to the *Guide for the Care and Use of Laboratory Animals*[46] and animal welfare regulations.[3,4] Husbandry included the use of ventilated microisolation caging (Lab Products, Seaford, DE), sterile cage setups with autoclaved hardwood bedding (Sani-Chip, Harlan Teklad, Madison, WI), and food (Rodent NIH-31 Autoclavable NA, Zeigler Brothers, Gardners, PA) and acidified water provided ad libitum. Room temperature was maintained at 20.0 to 23.3 °C, relative humidity between 30% and 50%, and light on a 14:10-h light:dark cycle. The colony sentinel program was tested quarterly and free of the following agents: mouse hepatitis virus, pneumonia virus of mice, Sendai virus, Theiler murine encephalomyelitis virus, mouse rotavirus, lymphocytic choriomeningitis virus, ectromelia virus, mouse cytomegalovirus, minute virus of mice, polyoma virus, reovirus 3, mouse adenovirus, rodent parvoviruses, *Mycoplasma pulmonis*, and cilia-associated respiratory bacillus. Hantavirus testing was performed once a year, and endoparasite and ectoparasite examination performed every 6 wk. Mouse norovirus and *Helicobacter* spp. were not excluded from the animal colony; therefore, mice were potentially infected with these agents.

Euthanasia of sick mice was performed through CO_2 overdose, according to the AVMA guidelines on euthanasia,[2] and complete necropsies performed immediately. Tissue samples from lesions and all major organs were collected and fixed in 10% neutral-buffered formalin. Fixed hearts were hemisected to expose all chambers and valves and then trimmed. Fixed tissue samples were embedded in paraffin, sectioned at 5 µm, and stained with hematoxylin and eosin for light microscopy examination. In addition, samples taken from the lesions were submitted to the NIH Division of Veterinary Resources (Bethesda, MD) Microbiology Laboratory for routine bacteriological culture, isolation, and sensitivity tests. Serum samples from selected cases were submitted to a reference commercial laboratory (Charles River Laboratories, Wilmington, MA) for antibody testing against potential known mouse viral pathogens. In selected cases, myocardium samples taken from the midsection of the left ventricular free wall were fixed in 2% glutaraldehyde and 1% paraformaldehyde and processed routinely for transmission electron microscopy. Briefly, postfixation the samples were washed with 0.1 M cacodylate buffer (pH 7.4), fixed with 1% OsO_4, washed again with cacodylate buffer, washed with water and placed in 1% uranyl acetate for one hour. The tissues were subsequently serially dehydrated in ethanol and propylene oxide and embedded in EMBed 812 resin (Electron Microscopy Sciences, Hatfield, PA). Thin sections (approximately 80 nm) were obtained by using an ultramicrotome (Leica, Deerfield, IL), placed onto 300-mesh copper grids, and stained with saturated uranyl acetate in 50% methanol and then with lead citrate. The grids were viewed by using an electron microscope (JEM-1200EXII, JEOL, Tokyo, Japan) at 80 kV, and images were recorded by using a mid-mounted, 10.5-MP, CCD camera (XR611M, Advanced Microscopy Techniques, Danvers, MA).

Results

Historically, spontaneous cardiomyopathy and atrial thrombosis have been low in the animal facility that housed the IL4 receptor α-deficient BALB/c mice. The 134 necropsies performed during the 2014 fiscal year (October 1 through September 30) included only 5 (3.7%) cases of cardiomyopathy or atrial thrombosis (or both), and the 186 necropsies performed during fiscal year 2015 included only 7 cases (3.8%). The number of new cases of either cardiomyopathy or atrial thrombosis (or both) was 12 (4.85%) among 247 necropsies during fiscal year 2016 and 17 (11.3%) among 150 necropsies during fiscal year 2017. Of the 29 cases of cardiomyopathy or atrial thrombosis (or both) during fiscal years 2016 and 2017, 21 (72.4%) were mice from the IL4 receptor α-deficient colony, prompting the current study. The affected strains, sex, age at clinical presentation, clinical signs, and gross and microscopic findings for each mouse are shown in Table 1. Clinically, affected mice had hunched posture, ruffled hair coat, decreased activity, and dyspnea and, in some cases, tachypnea.

At necropsy, 19 (90.5%) of the 21 mice had various degrees of cardiomegaly; 17 (89.5%) of the 19 with cardiomegaly had atrial thrombosis, with 16 (94.1%) of the 17 affecting the left atrium. The majority of the affected mice were males (n = 17; 80.9%); the remaining 4 (19.0%) were females. Age at clinical presentation ranged from 8 to 32 wk (mean, 22.7 wk). In some cases, all mice in a cage showed clinical signs of heart failure simultaneously. Grossly, in severe cases, the heart was markedly enlarged, occupying approximately 1/3 of the thoracic cavity. The left atrium was very large, containing a focally extensive tan area, and the ventricular walls were hypertrophied or, in some cases, were thin and the ventricular chambers dilated on sectioning (Figure 1 A through D). Heart weights in severe cases exceeded 0.4 g (1.8% of body weight; normal, approximately 0.5%). Thoracic effusion was noted in a few animals. No gross lesions were noted in other organs.

Microscopically, the tan mass found in some cases in the left atrial auricle was confirmed to be a chronic fibrin thrombus, with areas of mineralization and cartilage formation. The ventricular myocardium and interventricular septum showed hypertrophic cardiomyocytes, mild or occasional focal fibrosis, a few necrotic myocardial fibers, and cardiomyocyte disarray; on longitudinal sections, the intercalated disks in some cardiomyocytes appeared wider and several times thicker than in normal hearts (Figure 1 E through F). These changes appeared more severe in mice with marked ventricular chamber dilation and ventricular wall thinning. Occasional mild suppurative

Table 1. Cases of cardiac disease in a colony of IL4 receptor α-deficient BALB/c mice between November 2015 and September 2017

Strain	Sex	Age (wk)	Clinical signs	Gross lesions	Microscopic lesions
Il4ra$^{flox/flox}$	M	12	Hunched posture, ruffled hair coat, thin, lethargy, dyspnea	Left atrial thrombosis and dilation, moderate cardiomegaly	Organized fibrin thrombus with mineralization, cardiomyocyte hypertrophy with ID defects
Il4ra$^{flox/flox}$	F	8	Found dead	Left atrial thrombosis and dilation, mild cardiomegaly	Organized fibrin thrombus, mild ventricular fibroplasia and cardiomyocyte hypertrophy, mild hepatic fibrosis
Il4ra$^{flox/flox}$	F	8	Hunched posture, ruffled hair coat, lethargy, dyspnea	Left atrial thrombosis and dilation, mild cardiomegaly	Organized fibrin thrombus, mild ventricular fibroplasia and cardiomyocyte hypertrophy, mild hepatic fibrosis
Il4ra$^{flox/flox}$	F	28	Hunched posture, ruffled hair coat, thin, tachypnea	Left atrial thrombosis and dilation, mild cardiomegaly	Organized fibrin thrombus with chondroid metaplasia, cardiomyocyte hypertrophy with ID defects, pulmonary perivasculitis
Il4ra$^{flox/flox}$	F	12	Hunched posture, ruffled hair coat, thin, dyspnea	Left atrial thrombosis and dilation, marked cardiomegaly with left ventricular chamber dilation and wall thinning	Organized fibrin thrombus, cardiomyocyte hypertrophy with ID defects, pulmonary alveolar histiocytosis
Il4ra$^{flox/flox}$ *Krt19*$^{WT/cre\text{ERT}}$	M	28	Hunched posture, ruffled hair coat, dyspnea	Left atrial thrombosis and dilation, marked cardiomegaly	Organized fibrin thrombus with mineralization, cardiomyocyte hypertrophy with ID defects, pulmonary perivasculitis
Il4ra$^{flox/flox}$ *Krt19*$^{WT/cre\text{ERT}}$	M	32	Hunched posture, ruffled hair coat, tachypnea	Moderate cardiomegaly with dilated left atrium	Cardiomyocyte hypertrophy with ID defects, enteritis hyperplastic
Il4ra$^{flox/flox}$Rosa26$^{Brainbow\text{-}2.1/Brainbow\text{-}2.1}$	F	24	Hunched posture, ruffled hair coat, dyspnea	Left atrial thrombosis and dilation, marked cardiomegaly with left ventricular chamber dilation and wall thinning	Organized fibrin thrombus with mineralization and chondroid metaplasia, cardiomyocyte hypertrophy with ID defects, moderate acidophilic macrophage pneumonia
Il4ra$^{flox/flox}$Rosa26$^{Brainbow\text{-}2.1/Brainbow\text{-}2.1}$	M	20	Hunched posture, ruffled hair coat, dyspnea	Left atrial thrombosis and dilation, marked cardiomegaly, ventricular chamber dilation and wall thinning	Organized fibrin thrombus, cardiomyocyte hypertrophy with ID defects, left ventricular and interventricular septum contraction band necrosis, pulmonary intracapillary fibrin thrombi, type II pneumocyte hyperplasia and alveolar histiocytosis
Il4ra$^{flox/flox}$Rosa26$^{Brainbow\text{-}2.1/Brainbow\text{-}2.1}$	M	16	Hunched posture, ruffled hair coat, mild tachypnea	Mild cardiomegaly	Right ventricular epicardial mineralization, mild cardiomyocyte hypertrophy
Il4ra$^{flox/flox}$*Pdgfrb*$^{WT/cre}$	M	20	Hunched posture, ruffled hair coat, dyspnea	Left atrial thrombosis and dilation, moderate cardiomegaly	Small organized fibrin thrombus, right ventricle epicardial mineralization, cardiomyocyte hypertrophy with ID defects, myocardial apex mild fibrosis and atrophy, pulmonary alveolar histiocytosis with surfactant accumulation
Il4ra$^{flox/flox}$*Pdgfrb*$^{WT/cre}$	M	24	Hunched posture, ruffled hair coat, thin, dyspnea	Left atrial thrombosis and dilation, moderate cardiomegaly	Organized fibrin thrombus with mineralization, cardiomyocyte hypertrophy with ID defects, mild myocardial fibrosis, mild pulmonary interstitial fibrosis with occasional intracapillary fibrin thrombi

Table 1. Continued

Strain	Sex	Age (wk)	Clinical signs	Gross lesions	Microscopic lesions
Il4ra$^{flox/flox}$*Pdgfrb*$^{WT/cre}$	M	24	Hunched posture, ruffled hair coat, dyspnea	Left atrial thrombosis and dilation, moderate cardiomegaly with mild left ventricular chamber dilation	Organized fibrin thrombus with mineralization, cardiomyocyte hypertrophy with ID defects, pulmonary interstitial fibrosis
Il4ra$^{flox/flox}$*Pdgfrb*$^{WT/cre}$	M	24	Hunched posture, ruffled hair coat, dyspnea	Left atrial thrombosis and dilation, moderate cardiomegaly with mild left ventricular chamber dilation	Organized fibrin thrombus with mineralization, cardiomyocyte hypertrophy with ID defects, pulmonary interstitial fibrosis
Il4ra$^{flox/flox}$*Pdgfrb*$^{WT/cre}$	M	24	Hunched posture, ruffled hair coat, dyspnea	Left atrial thrombosis and dilation, moderate cardiomegaly with mild left ventricular chamber dilation	Organized fibrin thrombus with mineralization, cardiomyocyte hypertrophy with ID defects, pulmonary interstitial fibrosis with occasional intracapillary fibrin thrombi
Il4ra$^{flox/flox}$*Pdgfrb*$^{WT/cre}$	M	32	Hunched posture, ruffled hair coat, dyspnea	Left atrial thrombosis and dilation, marked cardiomegaly with left ventricular chamber dilation and wall thinning	Organized fibrin thrombus, cardiomyocyte hypertrophy with ID defects, cardiomyocyte necrosis, pulmonary interstitial fibrosis and intracapillary thrombi, type II pneumocyte hyperplasia
Il4ra$^{flox/flox}$*Lgr5*$^{WT/EGFP\text{-}IRES\text{-}creERT2}$	M	28	Hunched posture, ruffled hair coat, mild dyspnea	Left atrial thrombosis and dilation, moderate cardiomegaly with left ventricular dilation and wall thinning	Organized fibrin thrombus, cardiomyocyte hypertrophy with ID defects, pulmonary alveolar histiocytosis and pulmonary intracapillary thrombi with mild perivasculitis
Il4ra$^{flox/flox}$*Lgr5*$^{WT/EGFP\text{-}IRES\text{-}creERT2}$	M	28	Hunched posture, ruffled hair coat, tachypnea	Moderate cardiomegaly	Left ventricular hypertrophy, cardiomyocyte hypertrophy with ID defects, degeneration and fibrosis, pulmonary alveolar histiocytosis
Il4ra$^{flox/flox}$*Lgr5*$^{WT/EGFP\text{-}IRES\text{-}creERT2}$	M	28	Hunched posture, ruffled hair coat, tachypnea	Mild cardiomegaly	Myofiber degeneration and fibrosis, mild cardiomyocyte hypertrophy, pulmonary alveolar histiocytosis
Il4ra$^{flox/flox}$*Lgr5*$^{WT/EGFP\text{-}IRES\text{-}creERT2}$	F	20	Hunched posture, ruffled hair coat, thin, tachypnea	Left atrial thrombosis and dilation, marked cardiomegaly	Organized fibrin thrombus, cardiomyocyte hypertrophy with ID defects, pulmonary edema and alveolar histiocytosis
Il4ra$^{flox/flox}$*Krt19*$^{cre\text{ERT}/WT}$Rosa26$^{tdTomato/tdTomato}$	M	32	Hunched posture, ruffled hair coat, thin, lethargy, dyspnea	Right atrial thrombosis and dilation, marked cardiomegaly with ventricular chamber dilation and wall thinning	Organized fibrin thrombus, cardiomyocyte hypertrophy with ID defects, pulmonary alveolar histiocytosis, stomach mucosal ulcers, and renal tubular necrosis

ID, intercalated disk

inflammation of atrial myocardium was observed. Two mice had focally extensive epicardial mineralization of the right ventricle, but only one of them had atrial thrombosis. Contraction band necrosis was observed in one animal. No infectious agents were noted.

Microscopic lesions were found in other organs. Most commonly, pulmonary alveolar histiocytosis characterized by hemosiderin-laden alveolar macrophages were present diffusely in lung, consistent with left heart failure, along with fibrosis of alveolar septa with type II pneumocyte hyperplasia in a few cases. Pulmonary capillary fibrin thrombi were noted in 4 mice, these same animals also had left atrial thrombosis. Three mice had mild multifocal perivascular histiocytosis and lymphoid aggregates. The inflammatory cell aggregates were not associated with bronchioles. The cause of the perivasculitis in these 3 mice is unclear, given that bacterial cultures and serology testing for common viral agents were all negative, and microscopic examination did not reveal signs of a potential infectious agent. Two animals showed diffuse liver lipidosis and bile duct hyperplasia surrounded by fibrosis or focal areas of acute renal cortical tubular necrosis.

Bacterial cultures from heart samples were consistently negative. Serology panel testing for 24 known mouse pathogens also was negative. Because the clinical signs were an unexpected phenotype and extensive testing at necropsy (bacterial isolation by conventional methods, serology panels against known

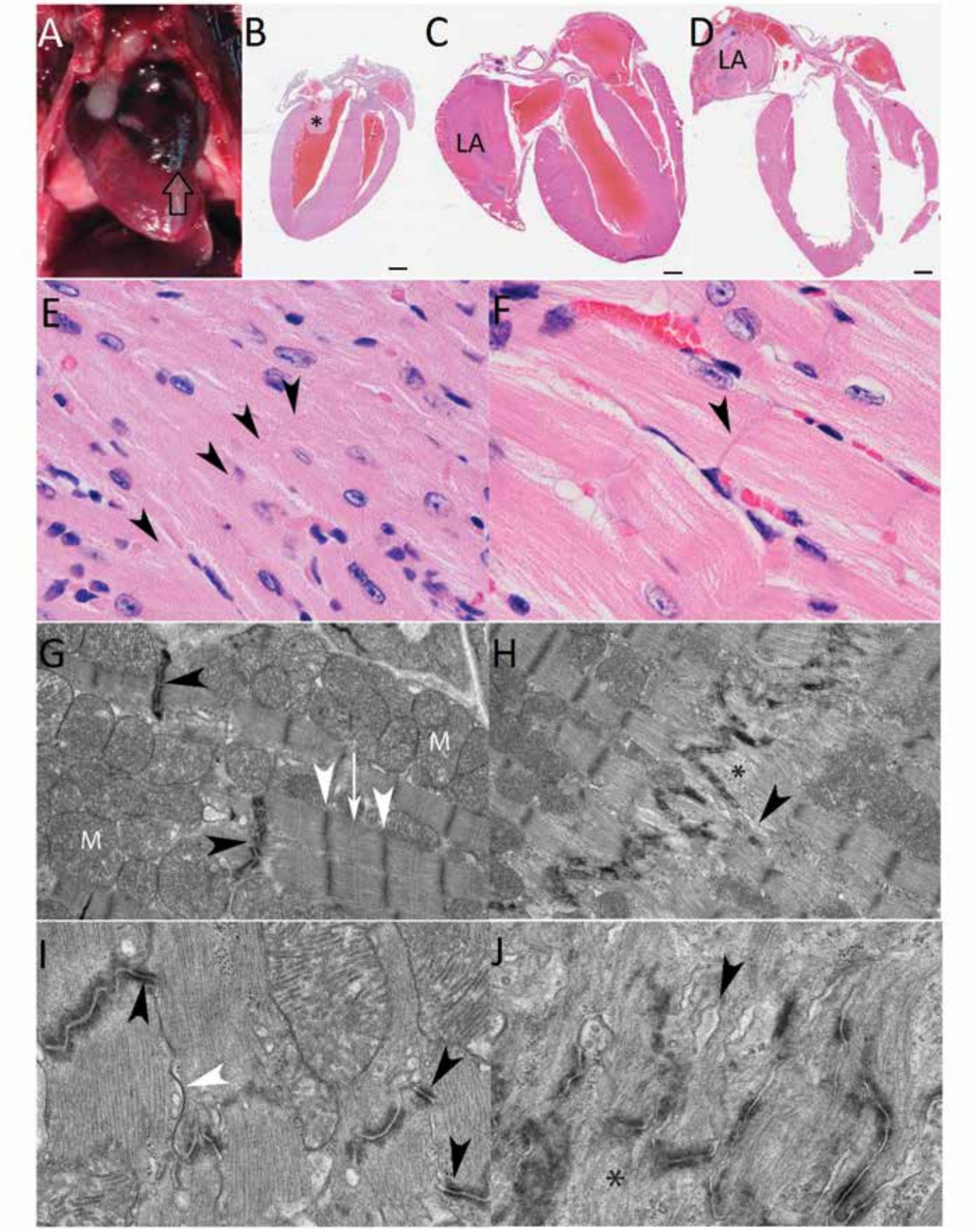

Figure 1. (A) Mouse, heart. Marked left atrial dilation (open arrow). (B) Mouse, heart. Low-power histologic longitudinal section showing a small fibrin thrombus (black asterisk) in the left ventricle chamber and attached to the mitral valve, but the heart is otherwise normal. (C) Mouse, heart. Low-power histologic longitudinal section showing marked thrombosis and dilation of the left atrium (LA) and left ventricle hypertrophy, with mild chamber dilation. (D) Mouse, heart. Low-power histologic longitudinal section showing marked thrombosis and dilation of the LA and marked ventricular dilation, with thinning of the left ventricular free wall. Hematoxylin and eosin stain; original magnification, 12.5×; bar,

mouse pathogens, and histologic examination by conventional light microscopy) failed to ascertain the etiology, heart tissue samples from 3 selected cases were processed for transmission electron microscopy. This examination did not reveal an infectious agent; however, the mice with cardiomegaly had structural defects of the intercalated disks characterized by unorganized and heavily convoluted arrangement with lower density and less prominent desmosomes and adherens junctions as compared with those of unaffected mice, giving the appearance of a thickened intercalated disk on light microscopy. Mitochondria appeared smaller and less numerous, and sarcomeres appeared thinner than in normal heart. In addition, the cardiomyocytes of the affected mice presented with widening of the intercellular space, myofibrillar lysis adjacent to intercalated disks, and increased number of endocytotic vesicles (Figure 1 G through J). Occasional sarcomere lysis with marked myofiber degeneration, vacuolation, accumulation of cell debris, and multiple whorls (myelin figures) was noted also.

Discussion

The increased incidence of cardiomyopathy and atrial thrombosis in an IL4 receptor α-deficient mice colony prompted us to do this retrospective study. Transmission electron microscopy of the myocardial cells in the affected animals showed the wider and thicker intercalated disks, noted on light microscopy, were results of the unorganized and heavily convoluted arrangement of the intercalated disks, with less dense and prominent desmosomes and adherens junctions. Widening of the intercellular space and myofibrillar lysis next to the intercalated disk were present also, along with occasional sarcomere lysis with marked myofiber degeneration, vacuolation, accumulation of cell debris, and myelin figures. The intercalated disk is responsible for the strong cell-to-cell adhesion, mechanosensing, and electrical signaling of cardiomyocytes.[20] It coordinates muscle contraction by coupling the electrical and mechanical connection between cardiac fibers with 3 main types of cell-to-cell contacts: desmosomes, gap junctions, and adherens junctions.[20] Typically, intercalated disk defects result in poor myocardial contraction, intracardiac blood stagnation, and consequently cardiac dilation, ultimately resulting in clinical signs of heart failure.[20,80]

A few genetically modified mice have been created as models of intercalated disk defects for the study of human disease conditions. These genetically modified mice show similarities to what we reported in the current study. Muscle LIM protein (MLP) knockout mice and tropomodulin-overexpressing transgenic (TOT) mice both develop dilated cardiomyopathy associated to altered expression levels of cytoskeletal proteins (either the lack of muscle LIM protein or an increased expression of tropomodulin) resulting in impaired myofibrillar function, physiologic stress, and altered appearance and composition of the intercalated disks showing a higher degree of convolution of the membrane at the intercalated disk, giving the impression of a broader region on light microscopy.[21] Mice carrying a deletion of the adhesive extracellular domain of the desmosomal cadherin desmoglein 2 develop arrhythmogenic right ventricular cardiomyopathy with ventricular dilation, fibrosis, and arrhythmia.[49] These mice have more severe defects at the intercalated disk level characterized by indistinguishable desmosomes, widening of the intercellular space, and even complete dissociation of intercalated disks.[49] Affected mice also showed disturbed sarcomere structure, altered Z-lines, multiple autophagic vacuoles, and swollen mitochondria.[49] On cardiomyocyte death, the tissue is repaired by connective tissue compromising even further heart function.[49] Cardiac-restricted myopalladin transgenic mice develop hypertrophic cardiomyopathy and disrupted intercalated disks, with disturbed expression of desmin, desmoplakin, connexin 43 and vinculin.[83] The Y20C mutation perturbs nuclear shuttling of myopalladin and leads to abnormal assembly of terminal Z-lines within the cardiac transitional junction and intercalated disk.[83] Transgenic mice with cardiac overexpression of mutant desmoglein 2 (Dsg2-N271S Tg-NS/L) develop intercellular space widening at the level of the intercalated disk and a concomitant reduction in action potential upstroke velocity as a consequence of lower Na^+ current density, leading to slowed conduction and increased arrhythmia susceptibility at disease stages preceding the onset of necrosis and replacement fibrosis.[85] In cardiomyopathic hamster models, although δ-sarcoglycan-deficient hamsters have altered sarcolemal structures, the cardiomyocytes of the UM-X7.1 hamster show highly convoluted and more electron-dense myocardial intercalated disks due to abnormally developed desmosomes with greater width, and myofibrillar loss at the adherens junction.[101] UM-X7.1 hamsters have reduced β-catenin expression that aggravates with age.[101]

In domestic animals, spontaneous intercalated disk defects have been described in boxer dogs with arrhythmogenic right ventricular cardiomyopathy.[78] Dogs with arrhythmogenic right ventricular cardiomyopathy had reduced numbers of desmosomes, adherens junctions, and gap junctions when compared with normal dogs.[78] In addition, the affected dogs had electron-dense material originating from the Z-line and extending into the sarcomere.[78] This last finding was not observed in the affected mice in the current study.

In humans, myocardial intercalated disk defects have been associated with mutations of desmosomal and α-catenin genes. These genes are found at high levels in myocardial tissues and contribute to strong cell-to-cell adhesion.[80] Electrical coupling of cardiac muscle can also be affected by intercalated disk defects and mutations in proteins that make up the myofibrils leading to hereditary cardiomyopathies.[80] The changes in cardiac

100 µm. (E). Mouse, heart. Photomicrograph showing normal myocardium with intercalated disks barely noticeable (black arrowheads). (F). Mouse, heart. Photomicrograph showing the myocardium of an affected animal with hypertrophy of individual cardiomyocytes and thickened intercalated disks (black arrowhead). Hematoxylin and eosin stain; magnification, 1000×. (G). Mouse, heart. Photomicrograph of a normal myocardial cell showing the intercalated disk (black arrowheads) connecting 2 cardiomyocytes. Note the step-ladder shaped arrangement of the intercalated disk. Numerous mitochondria (M) are normal. The Z-lines (white arrowheads) mark the lateral borders of a sarcomere with the M-band in the middle of the sarcomere (white arrow). (H). Mouse, heart. Photomicrograph of an abnormal myocardial cell intercalated disk showing unorganized and heavily convoluted arrangement with myofibrillar lysis next to the intercalated disk (black asterisk) and widening of the intercellular space (black arrow). Mitochondria appear smaller and less numerous, and sarcomeres appear thinner. Uranyl acetate and lead citrate stain; magnification, 5000×. (I). Mouse, heart. Photomicrograph showing details of a normal intercalated disk. Note the step-ladder shaped arrangement of the intercalated disk with desmosomes (black arrowheads), adherens junctions (less dense than desmosomes), and a gap junction (white arrowhead). (J). Mouse, heart. Photomicrograph showing an abnormal intercalated disk with unorganized arrangement, less dense desmosomes and adherences junctions, increased number of endocytotic vesicles, widening of the intercellular space (black arrowhead), and myofibrillar lysis next to the intercalated disk (black asterisk). Uranyl acetate and lead citrate stain; magnification, 10,000×.

cytoarchitecture that are seen in dilated cardiomyopathy are subtle and mainly affect the intercalated disks, with the plasma membrane between neighboring cardiomyocytes being more convoluted, resembling cell-to-cell contacts from aged hearts.[80] However, these subtle changes have a major effects on heart function, leading to a myocardium unable to contract with sufficient coordination and force to pump blood out of the cardiac chambers, thus predisposing to the development of intracardiac thrombi and eventual clinical signs of cardiac insufficiency.[20,80] Unfortunately, because the current study was a retrospective, postmortem study, echocardiography—necessary to evaluate heart function—was not performed in these mice.

The affected mice in the current study were all on a BALB/c background strain. Spontaneous epicardial mineralization is a common incidental finding in BALB/c mice, with lesions sometimes observed even in recently weaned animals.[9,33] The clinical significance of epicardial mineralization in BALB/c mice appears to be minimal, but its possible role in sudden death due to acute heart failure has not been adequately explored. Conversely, sudden death due to dystrophic intramural cardiac calcinosis has been described in C3H/OUJ mice fed high-fat purified diets.[23] In the current study, only 2 mice had epicardial mineralization of the right ventricle and only one of them had atrial thrombosis, consequently, epicardial mineralization did not appear to play a role in the development of atrial thrombosis in the animals in our study. Dilated cardiomyopathy is occasionally observed in aged laboratory mice, with atrial thrombosis being common in old female BALB/c mice.[28,68] BALB/c mice are highly susceptible to both infectious and noninfectious cardiomyopathy when compared with C57BL/6 mice.[79] BALB/c mice have a lower heart rate, an enlarged left ventricular chamber, a lower left ventricle ejection fraction and short fraction, and twice the amount of collagen in the left ventricle than age matched C57BL/6 mice.[79] However, dilated cardiomyopathy and atrial thrombosis in young mice is unusual. In the current study, the majority (80.9%) of the affected mice were males and younger than 6 mo at the time of clinical presentation. Similarly, in humans, the disease is usually diagnosed in young adults (20 to 25 y), and phenotypic expression is more common in men.[10] The difference in sex-associated presentation is believed to be due to a direct cardioprotective effect of estrogen in women. Estrogen has been shown to protect the myocardium against necrosis, apoptosis, fibrosis, hypertrophy, and inflammation, often preserving the heart ejection fraction.[10,50] This cardioprotective effect declines after menopause, as estrogen levels decline.[10,50]

Even though BALB/c mice are known to be susceptible to cardiomyopathy,[79] epicardial mineralization,[9,33] and cardiac dilation and thrombosis in older animals,[28,68] no reports describe intercalated disk defects as the cause of these lesions or address spontaneous intercalated disk defects in BALB/c mice. Furthermore, all affected mice in the current study were *Il4ra*$^{flox/flox}$, in which specific exons in the *ll4ra* locus are flanked by *loxP* sites (flox), allowing for the conditional deletion of IL4 receptor α on cell-specific expression of Cre recombinase but normal expression otherwise.[39,73] These mice have a functional phenotype of impaired IL4- and IL13-mediated activity but are not known to have defects affecting genes encoding for sarcomeric proteins, intracellular calcium regulation, expression of G protein-coupled receptors, or cardiac development.[73] Many of the strains in the current study incorporate Cre recombinase to induce conditional deletion of IL4 receptor α within selected cell types. The Cre–loxP-mediated recombination system is common gene editing tool in research. Sternberg and Hamilton were the first to describe a recombinase enzyme isolated from the P1 bacteriophage (a virus that infects bacteria) that recombines DNA fragments.[92] Although specific promoters and enhancers are used for narrowing the range of cells that express Cre, potential off-target Cre expression may confound interpretation of data.[63] Cre expression in vitro has been shown to reduce mammalian cell proliferation and result in aberrant DNA recombination and chromosomal defects.[56] In addition, cell-specific toxicity of Cre has been reported in various tissues, including cardiomyocytes.[82] Furthermore, high-level expression of Cre recombinase in the heart can cause dilated cardiomyopathy and premature death from congestive heart failure.[12] Other factors including genetic background, diet, and vivarium conditions may all play a role in the Cre-associated phenotype, given that cardiac outcomes are heavily influenced by genetic background in particular.[63] Nevertheless, *Il4ra*$^{flox/flox}$ mice have been used extensively in numerous studies and are not reported to have an untoward cardiac phenotype.[39,73] None of the promoters used to drive recombinase expression in the mice used in this study (*Pdgfrb*, *Krt19*, *Lgr5*) are reported to drive expression in cardiomyocytes; furthermore, several of the lines (*Il4ra*$^{flox/flox}$Rosa26$^{Brainbow\text{-}2.1/Brainbow\text{-}2.1}$, *Il4ra*$^{flox/flox}$) did not express Cre recombinase at all.

Whether the background strain and, potentially, the cre-loxP mediated recombination system used to create these mice contributed to the elevated incidence of cardiac dilatation and atrial thrombosis found in this colony is unknown. Given the backcrossing breeding scheme used in the colony, we cannot discount colonywide dissemination of a spontaneous mutation affecting the intercalated disk. However, because unintended Cre expression in heart or elsewhere can have untoward health effects, newly created genetically modified mice should always be carefully evaluated for off-target Cre expression and unintended downstream effects. The current report underscores the importance of carefully monitoring genetically modified mice for unexpected phenotypes that might result from spontaneous or unintended mutations or that may be related to background strains known to have aberrant cardiac phenotypes or unusual background pathology. Furthermore, transmission electron microscopy is an important tool for accurate diagnosis and phenotyping of genetically modified mice, particularly when evaluating previously unidentified cardiac abnormalities.

Acknowledgments

This study was supported by the Intramural Research Program of the National Institutes of Health, National Institute of Allergy and Infectious Diseases, Comparative Medicine Branch, and the Office of Research Services. We thank Dr Robert Thompson, Dr Thomas Wynn, and Dr Richard L Gieseck III from the Laboratory of Parasitic Diseases, NIAID, NIH, for usage of the animals in this report, Dr Robert Thompson for comments on the preliminary manuscript, and Ms Annie Merriweather and Mr Lucas Martin for histology support.

References

1. **Aherrahrou Z, Schlossarek S, Stoelting S, Klinger M, Geertz B, Weinberger F, Kessler T, Aherrahrou R, Moreth K, Bekeredjian R, Hrabě de Angelis M, Just S, Rottbauer W, Eschenhagen T, Schunkert H, Carrier L, Erdmann J.** 2015. Knock-out of nexilin in mice leads to dilated cardiomyopathy and endomyocardial fibroelastosis. Basic Res Cardiol **111:**6. https://doi.org/10.1007/s00395-015-0522-5.
2. **American Veterinary Medical Association**. [Internet]. 2013. Guidelines for the euthanasia of animals, 2013 edition. [Cited 15 May 2019]. Available at: https://www.avma.org/sites/default/files/resources/euthanasia.pdf
3. **Animal Welfare Act as Amended.** 2013. 7 USC § 2131–2159.
4. **Animal Welfare Regulations.** 2013. 9 CFR § 3.75–3.92.

5. **Arber S, Hunter JJ, Ross J Jr, Hongo M, Sansig G, Borg J, Perriard JC, Chien KR, Caroni P.** 1997. MLP-deficient mice exhibit a disruption of cardiac cytoarchitectural organization, dilated cardiomyopathy, and heart failure. Cell **88:**393–403. https://doi.org/10.1016/S0092-8674(00)81878-4.
6. **Bajusz E, Baker JR, Nixon CW, Homburger F.** 1969. Spontaneous, hereditary myocardial degeneration and congestive heart failure in a strain of Syrian hamsters. Ann N Y Acad Sci **156:**105–129. https://doi.org/10.1111/j.1749-6632.1969.tb16721.x.
7. **Baldeviano GC, Barin JG, Talor MV, Srinivasan S, Bedja D, Zheng D, Gabrielson K, Iwakura Y, Rose NR, Cihakova D.** 2010. Interleukin-17A is dispensable for myocarditis but essential for the progression to dilated cardiomyopathy. Circ Res **106:**1646–1655. https://doi.org/10.1161/CIRCRESAHA.109.213157.
8. **Barker N, van Es JH, Kuipers J, Kujala P, van den Born M, Cozijnsen M, Haegebarth A, Korving J, Begthel H, Peters PJ, Clevers H.** 2007. Identification of stem cells in small intestine and colon by marker gene Lgr5. Nature **449:**1003–1007. https://doi.org/10.1038/nature06196.
9. **Barthold SW, Griffey SM, Percy DH.** 2016. Index. p 371. Pathology of laboratory rodents and rabbits 4th edition. Ames (IA): Wiley–Blackwell. https://doi.org/10.1002/9781118924051
10. **Bennett RG, Haqqani HM, Berruezo A, Della Bella P, Marchlinski FE, Hsu CJ, Kumar S.** 2019. Arrhythmogenic cardiomyopathy in 2018–2019: ARVC/ALVC or Both? Heart Lung Circ **28:**164–177. https://doi.org/10.1016/j.hlc.2018.10.013.
11. **Bogomolovas J, Šimoliūnas E, Rinkūnaitė I, Smalinskaitė L, Podkopajev A, Bironaitė D, Weis CA, Marx A, Bukelskienė V, Gretz N, Grabauskienė V, Labeit D, Labeit S.** 2016. A novel murine model of parvovirus associated dilated cardiomyopathy induced by immunization with VP1-unique region of parvovirus B19. Biomed Res Int **2016:**1–9. https://doi.org/10.1155/2016/1627184.
12. **Buerger A, Rozhitskaya O, Sherwood MC, Dorfman AL, Bisping E, Abel ED, Pu WT, Izumo S, Jay PY.** 2006. Dilated cardiomyopathy resulting from high-level myocardial expression of Cre-recombinase. J Card Fail **12:**392–398. https://doi.org/10.1016/j.cardfail.2006.03.002.
13. **Bukowska A, Felgendreher M, Scholz B, Wolke C, Schulte JS, Fehrmann E, Wardelmann E, Seidl MD, Lendeckel U, Himmler K, Gardemann A, Goette A, Müller FU.** 2018. CREM-transgene mice: An animal model of atrial fibrillation and thrombogenesis. Thromb Res **163:**172–179. https://doi.org/10.1016/j.thromres.2017.07.033.
14. **Burek JD.** 1978. Cardiovascular system. p 75–94. In: Pathology of aging rats. Boca Raton (FL): CRC.
15. **Coral-Vazquez R, Cohn RD, Moore SA, Hill JA, Weiss RM, Davisson RL, Straub V, Barresi R, Bansal D, Hrstka RF, Williamson R, Campbell KP.** 1999. Disruption of the sarcoglycan-sarcospan complex in vascular smooth muscle: a novel mechanism for cardiomyopathy and muscular dystrophy. Cell **98:**465–474. https://doi.org/10.1016/S0092-8674(00)81975-3.
16. **Dambach DM, Lannon A, Sleeper MM, Buchanan J.** 1999. Familial dilated cardiomyopathy of young Portuguese water dogs. J Vet Intern Med **13:**65–71. https://doi.org/10.1111/j.1939-1676.1999.tb02167.x.
17. **Davenport WD Jr, Ball CR.** 1981. Diet-induced atrial endothelial damage—a scanning electron-microscopic study. Atherosclerosis **40:**145–152. https://doi.org/10.1016/0021-9150(81)90032-0.
18. **Duncker DJ, Bakkers J, Brundel BJ, Robbins J, Tardiff JC, Carrier L.** 2015. Animal and in silico models for the study of sarcomeric cardiomyopathies. Cardiovasc Res **105:**439–448. https://doi.org/10.1093/cvr/cvv006.
19. **Dunnick JK, Lieuallen W, Moyer C, Orzech D, Nyska A.** 2004. Cardiac damage in rodents after exposure to bis(2-chloroethoxy)methane. Toxicol Pathol **32:**309–317. https://doi.org/10.1080/01926230490431501.
20. **Ehler E.** 2016. Cardiac cytoarchitecture—why the "hardware" is important for heart function! Biochim Biophys Acta **1863: 7 Pt B:**1857–1863.
21. **Ehler E, Horowits R, Zuppinger C, Price RL, Perriard E, Leu M, Caroni P, Sussman M, Eppenberger HM, Perriard JC.** 2001. Alterations at the intercalated disk associated with the absence of muscle LIM protein. J Cell Biol **153:**763–772. https://doi.org/10.1083/jcb.153.4.763.
22. **Engelhardt S, Hein L, Wiesmann F, Lohse MJ.** 1999. Progressive hypertrophy and heart failure in β1-adrenergic receptor transgenic mice. Proc Natl Acad Sci U S A **96:**7059–7064. https://doi.org/10.1073/pnas.96.12.7059.
23. **Everitt JI, Olson LM, Mangum JB, Visek WJ.** 1988. High mortality with severe dystrophic cardiac calcinosis in C3H/OUJ mice fed high fat purified diets. Vet Pathol **25:**113–118. https://doi.org/10.1177/030098588802500202.
24. **Farris EJ, Yeakel EH, Seitner MM.** 1946. Ossifying cartilage and thrombi in the hearts of rats. Am J Pathol **22:**613–616.
25. **Fedak PWM, Smookler DS, Kassiri Z, Ohno N, Leco KJ, Verma S, Mickle DAG, Watson KL, Hojilla CV, Cruz W, Weisel RD, Li RK, Khokha R.** 2004. TIMP-3 Deficiency Leads to Dilated Cardiomyopathy. Circulation **110:**2401–2409. https://doi.org/10.1161/01.CIR.0000134959.83967.2D.
26. **Fentzke RC, Korcarz CE, Lang RM, Lin H, Leiden JM.** 1998. Dilated cardiomyopathy in transgenic mice expressing a dominant-negative CREB transcription factor in the heart. J Clin Invest **101:**2415–2426. https://doi.org/10.1172/JCI2950.
27. **Foo SS, Turner CJ, Adams S, Compagni A, Aubyn D, Kogata N, Lindblom P, Shani M, Zicha D, Adams RH.** 2006. Ephrin-B2 controls cell motility and adhesion during blood-vessel-wall assembly. Cell **124:**161–173. https://doi.org/10.1016/j.cell.2005.10.034.
28. **Fry RJ, Hamilton KH, Lisco H.** 1965. Thrombi in the left atrium of the heart in mice. Arch Pathol **80:**308–313.
29. **Fu Y, Eisen HJ.** 2018. Genetics of dilated cardiomyopathy. Curr Cardiol Rep **20:**121. https://doi.org/10.1007/s11886-018-1061-0.
30. **Fujihira S, Yamamoto T, Matsumoto M, Yoshizawa K, Oishi Y, Fujii T, Noguchi H, Mori H.** 1993. The high incidence of atrial thrombosis in mice given doxorubicin. Toxicol Pathol **21:**362–368. https://doi.org/10.1177/019262339302100403.
31. **Gao XM, Agrotis A, Autelitano DJ, Percy E, Woodcock EA, Jennings GL, Dart AM, Du XJ.** 2003. Sex hormones and cardiomyopathic phenotype induced by cardiac β2-adrenergic receptor overexpression. Endocrinology **144:**4097–4105. https://doi.org/10.1210/en.2002-0214.
32. **Gao XM, Dart AM, Dewar E, Jennings G, Du XJ.** 2000. Serial echocardiographic assessment of left ventricular dimensions and function after myocardial infarction in mice. Cardiovasc Res **45:**330–338. https://doi.org/10.1016/S0008-6363(99)00274-6.
33. **Glass AM, Coombs W, Taffet SM.** 2013. Spontaneous cardiac calcinosis in BALB/cByJ mice. Comp Med **63:**29–37.
34. **Grady RM, Teng H, Nichol MC, Cunningham JC, Wilkinson RS, Sanes JR.** 1997. Skeletal and cardiac myopathies in mice lacking utrophin and dystrophin: a model for Duchenne muscular dystrophy. Cell **90:**729–738. https://doi.org/10.1016/S0092-8674(00)80533-4.
35. **Gupta MK, Gulick J, James J, Osinska H, Lorenz JN, Robbins J.** 2013. Functional dissection of myosin binding protein C phosphorylation. J Mol Cell Cardiol **64:**39–50. https://doi.org/10.1016/j.yjmcc.2013.08.006.
36. **Hack AA, Ly CT, Jiang F, Clendenin CJ, Sigrist KS, Wollmann RL, McNally EM.** 1998. γ-Sarcoglycan deficiency leads to muscle membrane defects and apoptosis independent of dystrophin. J Cell Biol **142:**1279–1287. https://doi.org/10.1083/jcb.142.5.1279.
37. **Hambrook LE, Bennett PF.** 2012. Effect of pimobendan on the clinical outcome and survival of cats with non-taurine responsive dilated cardiomyopathy. J Feline Med Surg **14:**233–239. https://doi.org/10.1177/1098612X11429645.
38. **Heineke J, Wollert KC, Osinska H, Sargent MA, York AJ, Robbins J, Molkentin JD.** 2010. Calcineurin protects the heart in a murine model of dilated cardiomyopathy. J Mol Cell Cardiol **48:**1080–1087. https://doi.org/10.1016/j.yjmcc.2009.10.012.
39. **Herbert DR, Hölscher C, Mohrs M, Arendse B, Schwegmann A, Radwanska M, Leeto M, Kirsch R, Hall P, Mossmann H, Claussen B, Förster I, Brombacher F.** 2004. Alternative macrophage activation is essential for survival during schistosomiasis and down-modulates T helper 1 responses and immunopathology. Immunity **20:**623–635. https://doi.org/10.1016/S1074-7613(04)00107-4.

40. **Hirota H, Chen J, Betz UA, Rajewsky K, Gu Y, Ross J Jr, Müller W, Chien KR.** 1999. Loss of a gp130 cardiac muscle cell survival pathway is a critical event in the onset of heart failure during biomechanical stress. Cell **97:**189–198. https://doi.org/10.1016/S0092-8674(00)80729-1.
41. **Huang W, Liang J, Yuan CC, Kazmierczak K, Zhou Z, Morales A, McBride KL, Fitzgerald-Butt SM, Hershberger RE, Szczesna-Cordary D.** 2015. Novel familial dilated cardiomyopathy mutation in MYL2 affects the structure and function of myosin regulatory light chain. FEBS J **282:**2379–2393. https://doi.org/10.1111/febs.13286.
42. **Hunter EG, Hughes V, White J.** 1984. Cardiomyopathic hamsters, CHF 146 and CHF 147: a preliminary study. Can J Physiol Pharmacol **62:**1423–1428. https://doi.org/10.1139/y84-236.
43. **Ikeda Y, Martone M, Gu Y, Hoshijima M, Thor A, Oh SS, Peterson KL, Ross J Jr.** 2000. Altered membrane proteins and permeability correlate with cardiac dysfunction in cardiomyopathic hamsters. Am J Physiol Heart Circ Physiol **278:**H1362–H1370. https://doi.org/10.1152/ajpheart.2000.278.4.H1362.
44. **Ikeda Y, Ross J.** 2000. Models of dilated cardiomyopathy in the mouse and the hamster. Curr Opin Cardiol **15:**197–201. https://doi.org/10.1097/00001573-200005000-00013.
45. **Ikeda Y, Ross J.** 2011. Models of cardiac disease in the mouse, p 335–352. In: Cardiovascular physiology in the genetically engineered mouse. Boston (MA): Springer. https://doi.org/10.1007/978-1-4615-1653-8_21
46. **Institute for Laboratory Animal Research.** 2011. Guide for the care and use of laboratory animals, 8th ed, p 220. Washington (DC): National Academies Press.
47. **Iwase M, Uechi M, Vatner DE, Asai K, Shannon RP, Kudej RK, Wagner TE, Wight DC, Patrick TA, Ishikawa Y, Homcy CJ, Vatner SF.** 1997. Cardiomyopathy induced by cardiac Gs α overexpression. Am J Physiol **272:**H585–H589.
48. **Jones LR, Suzuki YJ, Wang W, Kobayashi YM, Ramesh V, Franzini-Armstrong C, Cleemann L, Morad M.** 1998. Regulation of Ca2+ signaling in transgenic mouse cardiac myocytes overexpressing calsequestrin. J Clin Invest **101:**1385–1393. https://doi.org/10.1172/JCI1362.
49. **Kant S, Krull P, Eisner S, Leube RE, Krusche CA.** 2012. Histological and ultrastructural abnormalities in murine desmoglein 2-mutant hearts. Cell Tissue Res **348:**249–259. https://doi.org/10.1007/s00441-011-1322-3.
50. **Kessler EL, Rivaud MR, Vos MA, van Veen TAB.** 2019. Sex-specific influence on cardiac structural remodeling and therapy in cardiovascular disease. Biol Sex Differ **10:**1–11. https://doi.org/10.1186/s13293-019-0223-0.
51. **Kim J, Lee K, Fujioka H, Tandler B, Hoppel CL.** 2018. Cardiac mitochondrial structure and function in tafazzin-knockdown mice. Mitochondrion **43:**53–62. https://doi.org/10.1016/j.mito.2018.10.005.
52. **Kishimoto C, Ochiai H, Sasayama S.** 1992. Intracardiac thrombus in murine Coxsackievirus B3 myocarditis. Heart Vessels **7:**76–81. https://doi.org/10.1007/BF01744452.
53. **Klevay LM.** 1985. Atrial thrombosis, abnormal electrocardiograms and sudden death in mice due to copper deficiency. Atherosclerosis **54:**213–224. https://doi.org/10.1016/0021-9150(85)90180-7.
54. **Kyu B, Matsumori A, Sato Y, Okada I, Chapman NM, Tracy S.** 1992. Cardiac persistence of cardioviral RNA detected by polymerase chain reaction in a murine model of dilated cardiomyopathy. Circulation **86:**522–530. https://doi.org/10.1161/01.CIR.86.2.522.
55. **Liu SK.** 1970. Acquired cardiac lesions leading to congestive heart failure in the cat. Am J Vet Res **31:**2071–2088.
56. **Loonstra A, Vooijs M, Beverloo HB, Allak BA, van Drunen E, Kanaar R, Berns A, Jonkers J.** 2001. Growth inhibition and DNA damage induced by Cre recombinase in mammalian cells. Proc Natl Acad Sci USA **98:**9209–9214. https://doi.org/10.1073/pnas.161269798.
57. **Lu WY, Bird TG, Boulter L, Tsuchiya A, Cole AM, Hay T, Guest RV, Wojtacha D, Man TY, Mackinnon A, Ridgway RA, Kendall T, Williams MJ, Jamieson T, Raven A, Hay DC, Iredale JP, Clarke AR, Sansom OW, Forbes SJ.** 2015. Hepatic progenitor cells of biliary origin with liver repopulation capacity. Nat Cell Biol **17:**971–983. https://doi.org/10.1038/ncb3203.
58. **Madisen L, Zwingman TA, Sunkin SM, Oh SW, Zariwala HA, Gu H, Ng LL, Palmiter RD, Hawrylycz MJ, Jones AR, Lein ES, Zeng H.** 2009. A robust and high-throughput Cre reporting and characterization system for the whole mouse brain. Nat Neurosci **13:**133–140. https://doi.org/10.1038/nn.2467.
59. **Maiellaro-Rafferty K, Wansapura JP, Mendsaikhan U, Osinska H, James JF, Taylor MD, Robbins J, Kranias EG, Towbin JA, Purevjav E.** 2013. Altered regional cardiac wall mechanics are associated with differential cardiomyocyte calcium handling due to nebulette mutations in preclinical inherited dilated cardiomyopathy. J Mol Cell Cardiol **60:**151–160. https://doi.org/10.1016/j.yjmcc.2013.04.021.
60. **Matsumori A.** 1992. Lessons from animal experiments in myocarditis. Herz **17:**107–111.
61. **McConnell BK, Jones KA, Fatkin D, Arroyo LH, Lee RT, Aristizabal O, Turnbull DH, Georgakopoulos D, Kass D, Bond M, Niimura H, Schoen FJ, Conner D, Fischman DA, Seidman CE, Seidman JG.** 1999. Dilated cardiomyopathy in homozygous myosin-binding protein-C mutant mice. J Clin Invest **104:**1235–1244. https://doi.org/10.1172/JCI7377.
62. **McConnell BK, Singh S, Fan Q, Hernandez A, Portillo JP, Reiser PJ, Tikunova SB.** 2015. Knock-in mice harboring a Ca^{2+} desensitizing mutation in cardiac troponin C develop early onset dilated cardiomyopathy. Front Physiol **6:**1–14. https://doi.org/10.3389/fphys.2015.00242.
63. **McLellan MA, Rosenthal NA, Pinto AR.** 2017. Cre-loxP-mediated recombination: general principles and experimental considerations. Curr Protoc Mouse Biol **7:**1–12. https://doi.org/10.1002/cpmo.22.
64. **McMartin DN.** 1977. Spontaneous atrial thrombosis in aged Syrian hamsters. I. Incidence and pathology. Thromb Haemost **38:**447–456. https://doi.org/10.1055/s-0038-1651480.
65. **McMartin DN, Dodds WJ.** 1982. Animal model of human disease: atrial thrombosis in aged Syrian hamsters. Am J Pathol **107:**277–279.
66. **Means AL, Xu Y, Zhao A, Ray KC, Gu G.** 2008. A CK19(CreERT) knockin mouse line allows for conditional DNA recombination in epithelial cells in multiple endodermal organs. Genesis **46:**318–323. https://doi.org/10.1002/dvg.20397.
67. **Megeney LA, Kablar B, Perry RL, Ying C, May L, Rudnicki MA.** 1999. Severe cardiomyopathy in mice lacking dystrophin and MyoD. Proc Natl Acad Sci USA **96:**220–225. https://doi.org/10.1073/pnas.96.1.220.
68. **Meier H, Hoag WG.** 1961. Studies on left auricular thrombosis in mice. Exp Med Surg **19:**317–322.
69. **Meurs KM, Lahmers S, Keene BW, White SN, Oyama MA, Mauceli E, Lindblad-Toh K.** 2012. A splice site mutation in a gene encoding for PDK4, a mitochondrial protein, is associated with the development of dilated cardiomyopathy in the Doberman pinscher. Hum Genet **131:**1319–1325. https://doi.org/10.1007/s00439-012-1158-2.
70. **Meurs KM, Miller MW, Wright NA.** 2001. Clinical features of dilated cardiomyopathy in Great Danes and results of a pedigree analysis: 17 cases (1990–2000). J Am Vet Med Assoc **218:**729–732. https://doi.org/10.2460/javma.2001.218.729.
71. **Meurs KM, Stern JA, Sisson DD, Kittleson MD, Cunningham SM, Ames MK, Atkins CE, DeFrancesco T, Hodge TE, Keene BW, Reina Doreste Y, Leuthy M, Motsinger-Reif AA, Tou SP.** 2013. Association of dilated cardiomyopathy with the striatin mutation genotype in boxer dogs. J Vet Intern Med **27:**1437–1440. https://doi.org/10.1111/jvim.12163.
72. **Milner DJ, Weitzer G, Tran D, Bradley A, Capetanaki Y.** 1996. Disruption of muscle architecture and myocardial degeneration in mice lacking desmin. J Cell Biol **134:**1255–1270. https://doi.org/10.1083/jcb.134.5.1255.
73. **Mohrs M, Ledermann B, Köhler G, Dorfmüller A, Gessner A, Brombacher F.** 1999. Differences between IL4- and IL4 receptor α-deficient mice in chronic leishmaniasis reveal a protective role for IL13 receptor signaling. J Immunol **162:**7302–7308.
74. **Nigro V, Okazaki Y, Belsito A, Piluso G, Matsuda Y, Politano L, Nigro G, Ventura C, Abbondanza C, Molinari AM, Acampora D, Nishimura M, Hayashizaki Y, Puca GA.** 1997. Identification of the

Syrian hamster cardiomyopathy gene. Hum Mol Genet **6:**601–607. https://doi.org/10.1093/hmg/6.4.601.

75. **Nishimura H, Okazaki T, Tanaka Y, Nakatani K, Hara M, Matsumori A, Sasayama S, Mizoguchi A, Hiai H, Minato N, Honjo T.** 2001. Autoimmune dilated cardiomyopathy in PD-1 receptor-deficient mice. Science **291:**319–322. https://doi.org/10.1126/science.291.5502.319.
76. **O'Sullivan ML, O'Grady MR, Pyle WG, Dawson JF.** 2011. Evaluation of 10 genes encoding cardiac proteins in Doberman Pinschers with dilated cardiomyopathy. Am J Vet Res **72:**932–939. https://doi.org/10.2460/ajvr.72.7.932.
77. **Owczarek-Lipska M, Mausberg TB, Stephenson H, Dukes-McEwan J, Wess G, Leeb T.** 2012. A 16-bp deletion in the canine *PDK4* gene is not associated with dilated cardiomyopathy in a European cohort of Doberman Pinschers. Anim Genet **44:**239. https://doi.org/10.1111/j.1365-2052.2012.02396.x.
78. **Oxford EM, Danko CG, Kornreich BG, Maass K, Hemsley SA, Raskolnikov D, Fox PR, Delmar M, Moïse NS.** 2011. Ultrastructural changes in cardiac myocytes from Boxer dogs with arrhythmogenic right ventricular cardiomyopathy. J Vet Cardiol **13:**101–113. https://doi.org/10.1016/j.jvc.2011.03.002.
79. **Peng H, Yang XP, Carretero OA, Nakagawa P, D'Ambrosio M, Leung P, Xu J, Peterson EL, González GE, Harding P, Rhaleb NE.** 2011. Angiotensin II-induced dilated cardiomyopathy in Balb/c but not C57BL/6J mice. Exp Physiol **96:**756–764. https://doi.org/10.1113/expphysiol.2011.057612.
80. **Perriard JC, Hirschy A, Ehler E.** 2003. Dilated cardiomyopathy: a disease of the intercalated disc? Trends Cardiovasc Med **13:**30–38. https://doi.org/10.1016/S1050-1738(02)00209-8.
81. **Philipp U, Vollmar A, Häggström J, Thomas A, Distl O.** 2012. Multiple loci are associated with dilated cardiomyopathy in Irish wolfhounds. PLoS One **7:**1–6. https://doi.org/10.1371/journal.pone.0036691.
82. **Pugach EK, Richmond PA, Azofeifa JG, Dowell RD, Leinwand LA.** 2015. Prolonged Cre expression driven by the α-myosin heavy chain promoter can be cardiotoxic. J Mol Cell Cardiol **86:**54–61. https://doi.org/10.1016/j.yjmcc.2015.06.019.
83. **Purevjav E, Arimura T, Augustin S, Huby AC, Takagi K, Nunoda S, Kearney DL, Taylor MD, Terasaki F, Bos JM, Ommen SR, Shibata H, Takahashi M, Itoh-Satoh M, McKenna WJ, Murphy RT, Labeit S, Yamanaka Y, Machida N, Park JE, Alexander PM, Weintraub RG, Kitaura Y, Ackerman MJ, Kimura A, Towbin JA.** 2012. Molecular basis for clinical heterogeneity in inherited cardiomyopathies due to myopalladin mutations. Hum Mol Genet **21:**2039–2053. https://doi.org/10.1093/hmg/dds022.
84. **Ramot Y, Nyska A.** 2007. Drug-induced thrombosis: experimental, clinical, and mechanistic considerations. Toxicol Pathol **35:**208–225. https://doi.org/10.1080/01926230601156237.
85. **Rizzo S, Lodder EM, Verkerk AO, Wolswinkel R, Beekman L, Pilichou K, Basso C, Remme CA, Thiene G, Bezzina CR.** 2012. Intercalated disc abnormalities, reduced Na+ current density, and conduction slowing in desmoglein-2 mutant mice prior to cardiomyopathic changes. Cardiovasc Res **95:**409–418. https://doi.org/10.1093/cvr/cvs219.
86. **Sakamoto A.** 2003. Molecular pathogenesis of severe cardiomyopathy in the TO-2 hamster. Exp Clin Cardiol **8:**143–146.
87. **Sakamoto A, Ono K, Abe M, Jasmin G, Eki T, Murakami Y, Masaki T, Toyo-oka T, Hanaoka F.** 1997. Both hypertrophic and dilated cardiomyopathies are caused by mutation of the same gene, δ-sarcoglycan, in hamster: an animal model of disrupted dystrophin-associated glycoprotein complex. Proc Natl Acad Sci USA **94:**13873–13878. https://doi.org/10.1073/pnas.94.25.13873.
88. **Shou W, Aghdasi B, Armstrong DL, Guo Q, Bao S, Charng MJ, Mathews LM, Schneider MD, Hamilton SL, Matzuk MM.** 1998. Cardiac defects and altered ryanodine receptor function in mice lacking FKBP12. Nature **391:**489–492. https://doi.org/10.1038/35146.
89. **Silber EN, Katz LN.** 1975. Thromboembolism, p 537–539. In: Heart disease. New York (NY): MacMillan.
90. **Snippert HJ, van der Flier LG, Sato T, van Es JH, van den Born M, Kroon-Veenboer C, Barker N, Klein AM, van Rheenen J, Simons BD, Clevers H.** 2010. Intestinal crypt homeostasis results from neutral competition between symmetrically dividing Lgr5 stem cells. Cell **143:**134–144. https://doi.org/10.1016/j.cell.2010.09.016.
91. **Stern JA, Ueda Y.** 2018. Inherited cardiomyopathies in veterinary medicine. Pflugers Arch **471:**745–753. 10.1007/s00424-018-2209-x.
92. **Sternberg N, Hamilton D.** 1981. Bacteriophage P1 site-specific recombination. I. Recombination between loxP sites. J Mol Biol **150:**467–486. https://doi.org/10.1016/0022-2836(81)90375-2.
93. **Sussman MA, Welch S, Cambon N, Klevitsky R, Hewett TE, Price R, Witt SA, Kimball TR.** 1998. Myofibril degeneration caused by tropomodulin overexpression leads to dilated cardiomyopathy in juvenile mice. J Clin Invest **101:**51–61. https://doi.org/10.1172/JCI1167.
94. **Tomioka N, Kishimoto C, Matsumori A, Kawai C.** 1985. Mural thrombi in mice with acute viral myocarditis. Jpn Circ J **49:**1277–1279. https://doi.org/10.1253/jcj.49.1277.
95. **Tomioka N, Kishimoto C, Matsumori A, Kawai C.** 1986. Mural thrombus in experimental viral myocarditis in mice: relation between thrombosis and congestive heart failure. Cardiovasc Res **20:**665–671. https://doi.org/10.1093/cvr/20.9.665.
96. **Tougas CL, Grindrod T, Cai LX, Alkassis FF, Kasahara H.** 2019. Heterozygous *Mylk3* knockout mice partially recapitulate human DCM with heterozygous *MYLK3* mutations. Front Physiol **10:**696. https://doi.org/10.3389/fphys.2019.00696.
97. **Van Sligtenhorst I, Ding ZM, Shi ZZ, Read RW, Hansen G, Vogel P.** 2011. Cardiomyopathy in α-kinase 3 (ALPK3)-deficient mice. Vet Pathol **49:**131–141. https://doi.org/10.1177/0300985811402841.
98. **Van Vleet JF, Ferrans VJ, Weirich WE.** 1981. Pathologic alterations in congestive cardiomyopathy of dogs. Am J Vet Res **42:**416–424.
99. **Wang J, Wilhelmsson H, Graff C, Li H, Oldfors A, Rustin P, Brüning JC, Kahn CR, Clayton DA, Barsh GS, Thorén P, Larsson NG.** 1999. Dilated cardiomyopathy and atrioventricular conduction blocks induced by heart-specific inactivation of mitochondrial DNA gene expression. Nat Genet **21:**133–137. https://doi.org/10.1038/5089.
100. **Wess G, Schulze A, Butz V, Simak J, Killich M, Keller LJ, Maeurer J, Hartmann K.** 2010. Prevalence of dilated cardiomyopathy in Doberman Pinschers in various age groups. J Vet Intern Med **24:**533–538. https://doi.org/10.1111/j.1939-1676.2010.0479.x.
101. **Yoshida M, Ohkusa T, Nakashima T, Takanari H, Yano M, Takemura G, Honjo H, Kodama I, Mizukami Y, Matsuzaki M.** 2011. Alterations in adhesion junction precede gap junction remodelling during the development of heart failure in cardiomyopathic hamsters. Cardiovasc Res **92:**95–105. https://doi.org/10.1093/cvr/cvr182.
102. **Yoshizawa K, Kissling GE, Johnson JA, Clayton NP, Flagler ND, Nyska A.** 2005. Chemical-induced atrial thrombosis in NTP rodent studies. Toxicol Pathol **33:**517–532. https://doi.org/10.1080/01926230591034429.